

# Expanded Analysis of Benzo[*a*]pyrene–DNA Adducts Formed in Vitro and in Mouse Skin: Their Significance in Tumor Initiation

Liang Chen,<sup>†</sup> Prabu D. Devanesan,<sup>†</sup> Sheila Higginbotham,<sup>†</sup> Freek Ariese,<sup>‡,§</sup>  
Ryszard Jankowiak,<sup>§</sup> Gerry J. Small,<sup>‡,§</sup> Eleanor G. Rogan,<sup>†</sup> and  
Ercole L. Cavalieri<sup>\*,†</sup>

*Eppley Institute for Research in Cancer, University of Nebraska Medical Center,  
600 South 42nd Street, Omaha, Nebraska 68198-6805, Department of Chemistry,  
Iowa State University, Ames, Iowa 50011, and Ames Laboratory, USDOE, Iowa State University,  
Ames, Iowa 50011*

Received January 2, 1996<sup>®</sup>

This paper reports expanded analyses of benzo[*a*]pyrene (BP)–DNA adducts formed in vitro by activation with horseradish peroxidase (HRP) or 3-methylcholanthrene-induced rat liver microsomes and in vivo in mouse skin. The adducts formed by BP are compared to those formed by BP-7,8-dihydrodiol and *anti*-BP diol epoxide (BPDE). First, activation of BP by HRP produced 61% depurinating adducts: 7-(benzo[*a*]pyrene-6-yl)guanine (BP-6-N7Gua), BP-6-C8Gua, BP-6-N7Ade, and the newly identified BP-6-N3Ade. As a standard, the last adduct was synthesized along with BP-6-N1Ade by electrochemical oxidation of BP in the presence of adenine. Second, identification and quantitation of BP–DNA adducts formed by microsomal activation of BP showed 68% depurinating adducts: BP-6-N7Ade, BP-6-N7Gua, BP-6-C8Gua, BPDE-10-N7Ade, and the newly detected BPDE-10-N7Gua. The stable adducts were mostly BPDE-10-N<sup>2</sup>dG (26%), with 6% unidentified. BPDE-10-N7Ade and BPDE-10-N7Gua were the depurinating adducts identified after microsomal activation of BP-7,8-dihydrodiol or direct reaction of *anti*-BPDE with DNA. In both cases, the predominant adduct was BPDE-10-N<sup>2</sup>dG (90% and 96%, respectively). Third, when mouse skin was treated with BP for 4 h, 71% of the total adducts were the depurinating adducts BP-6-N7Gua, BP-6-C8Gua, BP-6-N7Ade, and small amounts of BPDE-10-N7Ade and BPDE-10-N7Gua. These newly detected depurinating diol epoxide adducts were found in larger amounts when mouse skin was treated with BP-7,8-dihydrodiol or *anti*-BPDE. The stable adduct BPDE-10-N<sup>2</sup>dG was predominant, especially with *anti*-BPDE. Comparison of the profiles of DNA adducts formed by BP, BP-7,8-dihydrodiol, and *anti*-BPDE with their carcinogenic potency indicates that tumor initiation correlates with the levels of depurinating adducts, but not with stable adducts. Furthermore, the levels of depurinating adducts of BP correlate with mutations in the Harvey-*ras* oncogene in DNA isolated from mouse skin papillomas initiated by this compound [Chakravarti *et al.* (1995) *Proc. Natl. Acad. Sci. U.S.A.* **92**, 10422–10426]. The depurinating adducts formed by BP in mouse skin appear to be the key adducts leading to tumor initiation.

## Introduction

Formation of adducts of polycyclic aromatic hydrocarbons (PAH)<sup>1</sup> with DNA is the first critical event in tumor initiation (1, 2). Identification and quantitation of PAH–DNA adducts formed in vitro and/or in vivo have been reported for benzo[*a*]pyrene (BP) (3–6), 7,12-dimethyl-

benz[*a*]anthracene (7, 8), and dibenzo[*a,h*]pyrene (DB[*a,h*]P) (9). These adducts, which are formed by two major mechanisms of activation, one-electron oxidation and formation of diol epoxides, are either stable or depurinating adducts. The stable adducts remain in the DNA, unless repaired, and the depurinating adducts are lost from the DNA by cleavage of the glycosidic bond. Determination of the structure of DNA adducts provides information on the mechanism of activation, the type of DNA damage, and, eventually, the biological significance in terms of tumor initiation. In fact, a relationship has been established between Harvey-*ras* mutations in mouse skin papillomas and misreplication of apurinic sites generated by loss of depurinating PAH–DNA adducts (10).

Both in vitro and in vivo, BP predominantly forms depurinating adducts, which arise via the one-electron oxidation pathway (3–6). As reported here, two additional BP–DNA adducts, 3-(benzo[*a*]pyren-6-yl)Ade (BP-6-N3Ade) (Figure 1) and BP-6-N1Ade (Figure 2), have been synthesized. The BP-6-N3Ade adduct could be formed biologically since the analogous 3-(dibenzo[*a,h*]pyren-10-yl)adenine (DB[*a,h*]P-10-N3Ade) adduct has

\* To whom correspondence should be addressed.

<sup>†</sup> Eppley Institute for Research in Cancer.

<sup>‡</sup> Department of Chemistry, Iowa State University.

<sup>§</sup> Ames Laboratory, USDOE.

<sup>®</sup> Abstract published in *Advance ACS Abstracts*, June 15, 1996.

<sup>1</sup> Abbreviations: *anti*-BPDE, (±)-benzo[*a*]pyrene *trans*-7,8-dihydrodiol 9,10-epoxide (*anti*); BP, benzo[*a*]pyrene; BP-6-C8Gua, 8-(benzo[*a*]pyren-6-yl)guanine; BP-6-N1Ade, 1-(benzo[*a*]pyren-6-yl)adenine; BP-6-N3Ade, 3-(benzo[*a*]pyren-6-yl)adenine; BP-6-N7Ade, 7-(benzo[*a*]pyren-6-yl)adenine; BP-6-N7Gua, 7-(benzo[*a*]pyren-6-yl)guanine; BPDE-10-N7Ade, 10-(adenin-7-yl)-7,8,9-trihydroxy-7,8,9,10-tetrahydrobenzo[*a*]pyrene; BPDE-10-N7Gua, 10-(guanin-7-yl)-7,8,9-trihydroxy-7,8,9,10-tetrahydrobenzo[*a*]pyrene; COSY, two-dimensional chemical shift correlation spectroscopy; dA, deoxyadenosine; DB[*a,h*]P, dibenzo[*a,h*]pyrene; DB[*a,h*]P-10-N3Ade, 3-(dibenzo[*a,h*]pyren-10-yl)adenine; dG, deoxyguanosine; DMF, dimethylformamide; FLNS, fluorescence line-narrowing spectroscopy; HRP, horseradish peroxidase; 3-MC, 3-methylcholanthrene; Me<sub>2</sub>SO, dimethyl sulfoxide; NOE, nuclear Overhauser effect; PAH, polycyclic aromatic hydrocarbon(s); PDA, photodiode array.

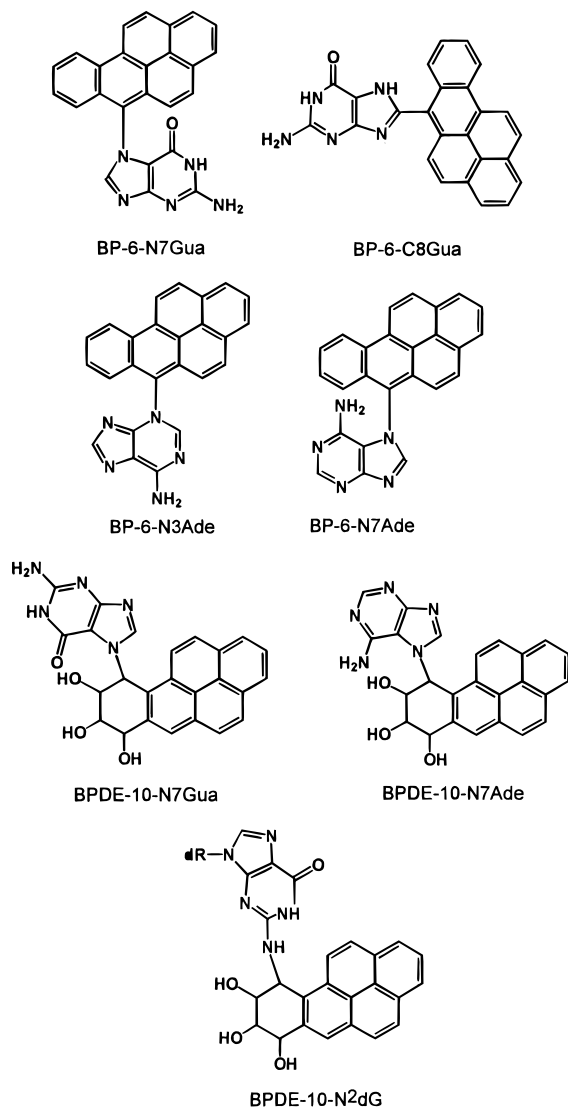


**Figure 1.** Structures of BP–DNA adducts formed biologically.

been found to be one of the major depurinating adducts formed by cytochrome P450 activation of DB[*a*,*l*]P in vitro (9). In addition, improvements in our technology for analyzing depurinating adducts have allowed us to determine the presence of two depurinating BP–DNA adducts formed via the diol epoxide pathway: 10-(adenin-7-yl)-7,8,9-trihydroxy-7,8,9,10-tetrahydrobenzo[*a*]pyrene (BPDE-10-N7Ade) and 10-(guanin-7-yl)-7,8,9-trihydroxy-7,8,9,10-tetrahydrobenzo[*a*]pyrene (BPDE-10-N7Gua) (Figure 1). This paper reports expanded analyses of BP–DNA adducts formed in vitro by 3-methylcholanthrene (3-MC)-induced rat liver microsomes or horseradish peroxidase (HRP) and in vivo in mouse skin. In addition, the adducts formed by BP-7,8-dihydrodiol and *anti*-BP diol epoxide (*anti*-BPDE) are determined and compared to those formed by BP itself.

The profile of possible depurinating adducts formed by BP with DNA now appears to be complete. This information is critical for identifying the adducts that play a significant role in tumor initiation by BP, BP-7,8-dihydrodiol, and *anti*-BPDE.

### Experimental Procedures

**Caution.** The following chemicals are hazardous and should be handled carefully in accordance with NIH guidelines (11): BP, BP-7,8-dihydrodiol, and *anti*-BPDE.

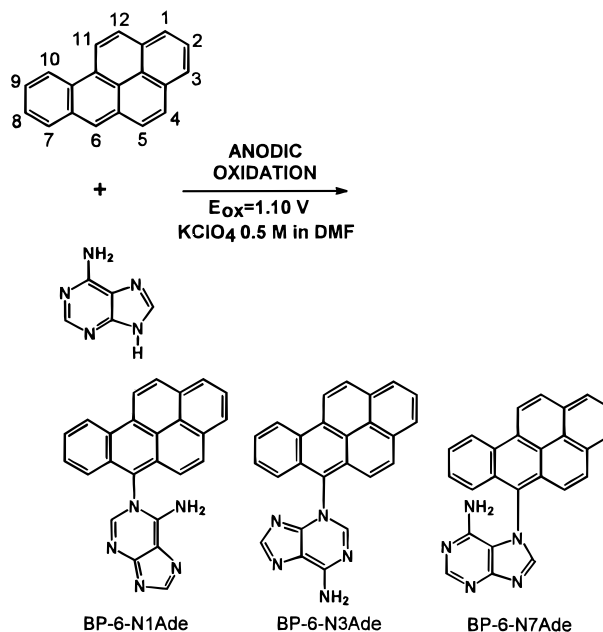


**Figure 2.** Electrochemical oxidation of BP in the presence of adenine.

**(A) General Procedures. Materials.** BP (Eastman, Rochester, NY) was available in our laboratory and was purified by column chromatography on aluminum oxide and elution with benzene/hexane (1:1). The product was recrystallized from benzene/hexane (mp 177–178 °C). 8-(Benzo[*a*]pyren-6-yl)guanine (BP-6-C8Gua), 7-(benzo[*a*]pyren-6-yl)guanine (BP-6-N7Gua), and 7-(benzo[*a*]pyren-6-yl)adenine (BP-6-N7Ade) (Figure 1) were synthesized by anodic oxidation of BP in the presence of deoxyguanosine (dG) or deoxyadenosine (dA) (3, 12). BPDE-10-N7Ade and BPDE-10-N7Gua were prepared by chemical reaction of *anti*-BPDE with dA or dG (12).

[<sup>3</sup>H]BP (sp act. 550 Ci/mol) was purchased from Amersham (Arlington Heights, IL), whereas [<sup>3</sup>H]-(*±*)-*trans*-BP-7,8-dihydrodiol (sp act. 767 Ci/mol) and [<sup>3</sup>H]-(*±*)-*r-r*,*t-t*-dihydroxy-*t*-9,10-epoxy-7,8,9,10-tetrahydro-BP (*anti*) (sp act. 1380 Ci/mol) were purchased from the NCI Chemical Carcinogen Repository (Bethesda, MD). [<sup>3</sup>H]BP was used at a specific activity of 400 Ci/mol; [<sup>3</sup>H]BP-7,8-dihydrodiol at 330 Ci/mol; and [<sup>3</sup>H]-*anti*-BPDE at 210 Ci/mol.

**HPLC.** Analytical HPLC was conducted on a Waters 600E solvent delivery system equipped with a Waters 700 WISP autoinjector. Effluents were monitored for UV absorbance (254 nm) with a Waters 996 photodiode array (PDA) detector. Biological samples were also monitored for radioactivity with an A250 series Radiomatic Flo-one/Beta radiation monitor (Radiomatic, Tampa, FL) and for fluorescence with a Jasco FP-920 fluorescence monitor. Separations were conducted on a YMC (YMC, Wilmington, NC) ODS-AQ 5 μm column (6 × 250 mm). Preparative HPLC separations were conducted on a YMC ODS-AQ 5 μm column (20 × 250 mm).

**UV.** UV absorbance spectra were recorded during HPLC separations with a Waters 990 PDA detector.

**NMR.** Proton and homonuclear two-dimensional chemical shift correlation spectroscopy (COSY) NMR spectra were recorded on a Varian Unity 500 at 499.835 MHz in deuterated dimethyl sulfoxide (Me<sub>2</sub>SO-*d*<sub>6</sub>) at 30 °C. Chemical shifts (δ) are reported relative to Me<sub>2</sub>SO (2.49 ppm), and the coupling constants (*J*) are given in hertz. Nuclear Overhauser effect (NOE) spectra were recorded in Me<sub>2</sub>SO-*d*<sub>6</sub> at 25 °C.

**MS.** Mass spectrometry experiments were performed on a Kratos MS-50 triple-analyzer tandem mass spectrometer in the laboratory of Dr. Michael Gross, Department of Chemistry, Washington University, St. Louis, MO.

**Fluorescence Line-Narrowing Spectroscopy (FLNS).** Samples were cooled in a double-nested glass cryostat with quartz optical windows. For selective excitation, a Lambda

Physik Lextra 100 excimer laser/FL-2002 dye laser system was used. Adduct samples were probed with the laser under non-line-narrowing conditions ( $77\text{ K}$ ,  $S_2 \leftarrow S_0$  excitation) for purity checking and under line-narrowing conditions ( $4.2\text{ K}$ ,  $S_1 \leftarrow S_0$  excitation) for fingerprint identification. Fluorescence was dispersed by a McPherson 2061 1-m monochromator (resolution for FLN experiments,  $0.08\text{ nm}$ ) and detected with a Princeton Instruments IRY-1024/GRB intensified PDA. For time-resolved detection (to reject scattered light) a Princeton Instruments FG-100 high-voltage pulse generator was used. The detector delay and gate width were  $20/100\text{ ns}$  for one-electron oxidation adducts (BP chromophores) and  $20/400\text{ ns}$  for BPDE adducts (pyrene chromophores).

**(B) Electrochemical Synthesis of Adducts.** The electrochemical reaction of BP with dA or dG was conducted as previously described (3, 12). The oxidation potential used for the synthesis of BP adducts was  $1.10\text{ V}$ , slightly less than its anodic peak potential of  $1.12\text{ V}$ , as measured by cyclic voltammetry (Model CV27, Bioanalytical Systems, Lafayette, IN) (13). Since all deoxyribonucleosides and adenine (Ade) have anodic peak potentials  $>1.2\text{ V}$ , none of the nucleosides were oxidized at this potential.

Electrochemical reaction of BP with Ade (1:30 molar ratio) was conducted in dimethylformamide (DMF), containing  $0.5\text{ M}$   $\text{KClO}_4$ , with consumption of  $1.6$  equiv of charge. Solvent was removed under vacuum at the end of the reaction. The solid residue ( $\text{KClO}_4$ ) was extracted four times with a mixture of ethanol/chloroform/acetone (2:1:1), the resulting extract filtered through a Whatman No. 1 fluted filter, and the filtrate evaporated under vacuum. The residue was dissolved in  $3\text{ mL}$  of  $\text{Me}_2\text{SO}$ , passed through a  $0.45\text{-}\mu\text{m}$  filter, and analyzed by HPLC. The column was eluted with  $30\%$   $\text{CH}_3\text{CN}$  in  $\text{H}_2\text{O}$  for  $5\text{ min}$ , followed by a convex (CV5) gradient to  $100\%$   $\text{CH}_3\text{CN}$  in  $80\text{ min}$  at a flow rate of  $1\text{ mL/min}$ . The adducts were isolated by preparative HPLC by eluting the column with  $55\%$   $\text{CH}_3\text{CN}$  in  $\text{H}_2\text{O}$  for  $5\text{ min}$ , followed by a convex (CV5) gradient to  $100\%$   $\text{CH}_3\text{CN}$  in  $80\text{ min}$  at a flow rate of  $6\text{ mL/min}$ . BP-6-N1Ade was found to behave differently from other adducts, eluting as a broad peak with no definite retention time in both  $\text{CH}_3\text{CN}/\text{H}_2\text{O}$  and  $\text{CH}_3\text{OH}/\text{H}_2\text{O}$  gradients. However, it was isolated at a consistent retention time by eluting the column with  $65\%$   $\text{C}_2\text{H}_5\text{-OH}/\text{CH}_3\text{CN}$  (3:1) in  $\text{H}_2\text{O}$  for  $15\text{ min}$ , followed by a linear gradient to  $100\%$   $\text{C}_2\text{H}_5\text{OH}/\text{CH}_3\text{CN}$  (3:1) in  $40\text{ min}$  at a flow rate of  $1\text{ mL/min}$ . The three products, BP-6-N1Ade, BP-6-N3Ade, and BP-6-N7Ade, were obtained in yields of  $52\%$ ,  $5.6\%$ , and  $1.7\%$ , respectively. The two new products, BP-6-N3Ade and BP-6-N1Ade, were characterized by UV, NMR, and mass spectrometry.

**BP-6-N3Ade:** UV:  $\lambda_{\text{max}}$  (nm) 256, 267, 290, 302, 359, 377, 397, 407;  $^1\text{H NMR}$ :  $\delta$  7.27 (d, 1H,  $J_{4,5} = 9.5\text{ Hz}$ , 5-H), 7.45 (d, 1H,  $J_{7,8} = 8.5\text{ Hz}$ , 7-H), 7.59 [bs, 2H, 6-NH<sub>2</sub> (Ade)], 7.81 (t, 1H,  $J_{7,8} = 8.5\text{ Hz}$ ,  $J_{8,9} = 8.5\text{ Hz}$ , 8-H), 7.96 (t, 1H,  $J_{8,9} = 8.5\text{ Hz}$ ,  $J_{9,10} = 8.5\text{ Hz}$ , 9-H), 7.98 [s, 1H, 8-H (Ade)], 8.08 (d, 1H,  $J_{4,5} = 9.5\text{ Hz}$ , 4-H), 8.14 (dd, 1H,  $J_{1,2} = 7.5\text{ Hz}$ ,  $J_{2,3} = 7.5\text{ Hz}$ , 2-H), 8.30 (d, 1H,  $J_{2,3} = 7.5\text{ Hz}$ , 3-H), 8.51 (d, 1H,  $J_{1,2} = 7.5\text{ Hz}$ , 1-H), 8.60 [s, 1H, 2-H (Ade)], 8.63 (d, 1H,  $J_{11,12} = 9.5\text{ Hz}$ , 12-H), 9.41 (d, 1H,  $J_{9,10} = 8.5\text{ Hz}$ , 10-H), 9.42 (d, 1H,  $J_{11,12} = 9.5\text{ Hz}$ , 11-H); MS:  $(\text{M} + 1)^+$   $\text{C}_{25}\text{H}_{16}\text{N}_5\text{O}_4$  386.1408 (calcd 386.1406).

**BP-6-N1Ade:** UV:  $\lambda_{\text{max}}$  (nm) 256, 267, 290, 303, 359, 379, 398, 408;  $^1\text{H NMR}$ :  $\delta$  7.33 (d, 1H,  $J_{4,5} = 9.5\text{ Hz}$ , 5-H), 7.52 (d, 1H,  $J = 8.5\text{ Hz}$ , 7-H), 7.60 [s, 1H, 8-H (Ade)], 7.81 (dd, 1H,  $J_{7,8} = 8.5\text{ Hz}$ ,  $J_{8,9} = 8.5\text{ Hz}$ , 8-H), 7.97 (dd, 1H,  $J_{8,9} = 8.5\text{ Hz}$ ,  $J_{9,10} = 8.5\text{ Hz}$ , 9-H), 8.10 (d, 1H,  $J_{4,5} = 9.5\text{ Hz}$ , 4-H), 8.15 (dd, 1H,  $J_{1,2} = 7.5\text{ Hz}$ ,  $J_{2,3} = 7.5\text{ Hz}$ , 2-H), 8.31 (d, 1H,  $J_{2,3} = 7.5\text{ Hz}$ , 3-H), 8.35 [bs, 1H, 6-NH (Ade)], 8.45 [bs, 1H, 6-NH (Ade)], 8.52 (d, 1H,  $J_{1,2} = 7.5\text{ Hz}$ , 1-H), 8.65 (d, 1H,  $J_{11,12} = 9.5\text{ Hz}$ , 12-H), 8.68 [s, 1H, 2-H (Ade)], 9.41 (d, 1H,  $J_{9,10} = 8.5\text{ Hz}$ , 10-H), 9.42 (d, 1H,  $J_{11,12} = 9.5\text{ Hz}$ , 11-H); MS:  $(\text{M} + 1)^+$   $\text{C}_{25}\text{H}_{16}\text{N}_5\text{O}_4$  386.1406 (calcd 386.1406).

**(C) Binding of PAH to DNA in Vitro.** [ $^3\text{H}$ ]BP ( $80\text{ }\mu\text{M}$ ) and [ $^3\text{H}$ ]BP-7,8-dihydrodiol ( $80\text{ }\mu\text{M}$ ) were bound to DNA in reactions catalyzed by 3-MC-induced rat liver microsomes (4, 5), and [ $^3\text{H}$ ]BP was also bound to DNA by HRP (3). *anti*-BPDE was bound

to DNA in a mixture containing  $2.6\text{ mM}$  calf thymus DNA in  $150\text{ mM}$  Tris-HCl ( $\text{pH } 7.5$ ),  $150\text{ mM}$  KCl,  $5\text{ mM}$   $\text{MgCl}_2$ , and  $80\text{ }\mu\text{M}$  [ $^3\text{H}$ ]-*anti*-BPDE. All of the reactions were  $15\text{ mL}$  in volume; they were incubated for  $30\text{ min}$  at  $37\text{ }^\circ\text{C}$ .

At the end of the reaction, a  $1\text{-mL}$  aliquot of the mixture was used to determine the amount of stable DNA adducts by the  $\text{P}_1$ -nuclease-modified  $^{32}\text{P}$ -postlabeling method, as previously described (14). The DNA from the remaining  $14\text{-mL}$  mixture was precipitated with 2 volumes of absolute ethanol, and the supernatant was used to identify and quantify the depurinating adducts by HPLC and FLNS.

**(D) Binding of BP, BP-7,8-dihydrodiol, and BPDE to Mouse Skin DNA.** Groups of eight female Swiss mice (8 weeks old, Eppley Colony) were treated on an area of shaved dorsal skin with  $200\text{ nmol}$  of tritiated BP, BP-7,8-dihydrodiol, or *anti*-BPDE in  $50\text{ }\mu\text{L}$  of acetone (6). The mice were killed after  $4\text{ h}$ , and the treated area was excised. Epidermis from each group was prepared, pooled, ground in liquid  $\text{N}_2$ , and split into two equal samples weighing approximately  $1\text{ g}$ . One was used to purify the DNA and to analyze the stable adducts by the  $^{32}\text{P}$ -postlabeling method. The other was Soxhlet-extracted for  $48\text{ h}$  with  $\text{CHCl}_3/\text{CH}_3\text{OH}$  (1:1) to recover the depurinating adducts, and the adducts were analyzed by HPLC and FLNS. The amount of DNA in each sample of ground epidermis was determined by the diphenylamine reaction (15) to be  $8.5 \pm 0.4\text{ mmol}$  of DNA-P/g of epidermis.

**(E) Analysis of Depurinating Adducts by HPLC and FLNS.** The supernatant from each binding reaction (in vitro) or the extract of the epidermis (in vivo), containing depurinating adducts and metabolites, was evaporated to dryness under vacuum, and the residue was dissolved in  $\text{Me}_2\text{SO}/\text{CH}_3\text{OH}$  (1:1). After sonication to enhance solubilization, the undissolved residue was removed by centrifugation. The depurinating adducts were analyzed by HPLC as previously described (5, 6). In the first experiment, the depurinating adducts were identified by HPLC in both  $\text{CH}_3\text{OH}/\text{H}_2\text{O}$  and  $\text{CH}_3\text{CN}/\text{H}_2\text{O}$  gradients in the presence of added authentic adducts. In the second experiment, the adducts eluting at the respective retention times of the authentic adducts were collected for identification by FLNS. For each peak, three fractions were collected (early, mid, and late), to assure by FLNS that the peak was homogeneous.

For FLN identification of collected HPLC fractions, the samples were dried in a Speedvac and redissolved in  $60\text{ }\mu\text{L}$  of a glass-forming solvent mixture with the help of sonication. The solvent system employed was water/glycerol/ethanol (40:40:20) for BP one-electron oxidation adducts or water/glycerol (50:50) for BPDE adducts. Aliquots ( $30\text{ }\mu\text{L}$ ) were transferred to  $2\text{ mm}$  i.d. quartz tubes and sealed with a rubber septum. Low-temperature fluorescence spectra were recorded using the apparatus described above. A detailed discussion on the use of fluorescence line-narrowing spectroscopy for the fingerprint identification of carcinogen-DNA adducts has been presented by Jankowiak and Small (16, 17).

**(F) Calculation of Adduct Levels.** The depurinating adducts were quantitated by counting radioactivity as previously described (5, 6). Each of the peaks eluting at the same time as an authentic adduct in HPLC using the  $\text{CH}_3\text{OH}/\text{H}_2\text{O}$  gradient was collected and counted. These peaks were then reinjected individually in an  $\text{CH}_3\text{CN}/\text{H}_2\text{O}$  gradient, and the percentage of the injected radioactivity eluting at the same time as the authentic adduct was measured and calculated using the radiation flow monitor. The total amount of each of the adducts was calculated from the specific activity of the PAH and normalized to the amount of DNA used in the reaction or calculated from the weight of the mouse epidermis sample. The amount of stable adducts was calculated by the  $^{32}\text{P}$ -postlabeling method as previously described (5, 6).

## Results and Discussion

**Structure Determination of Adducts Formed by Electrochemical Oxidation of BP in the Presence of Adenine.** Adducts of BP and deoxyribonucleosides

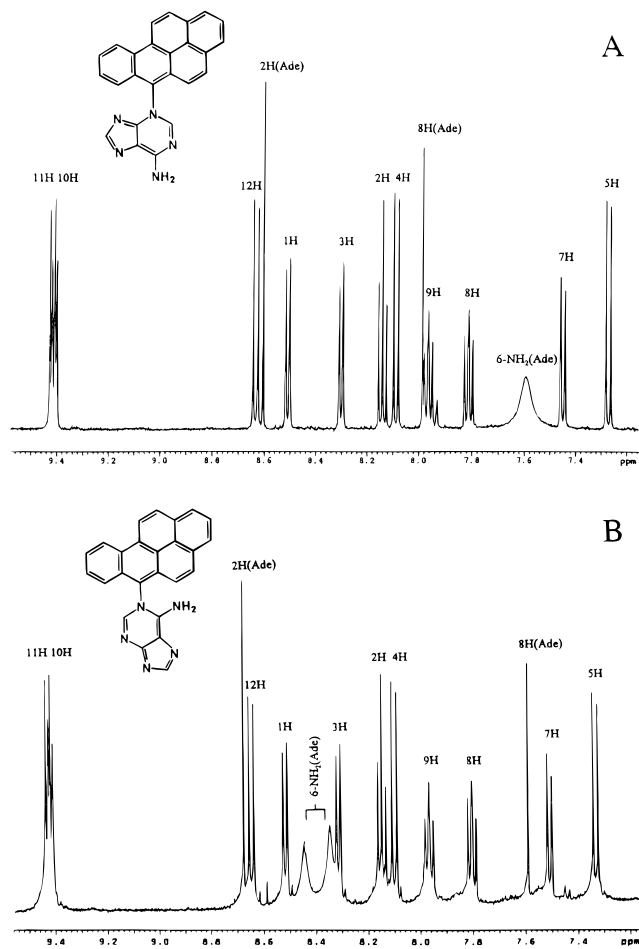


**Figure 3.** NMR spectra of (A) BP-6-N3Ade and (B) BP-6-N1Ade.

formed by electrochemical oxidation were previously synthesized (3, 12). Anodic oxidation of BP and dG afforded four primary adducts, BP-6-N7Gua, BP-6-C8dG, and trace amounts of BP-6-N<sup>2</sup>dG and BP-6-N3dG, as well as a secondary adduct, BP-6-C8Gua (Figure 1). Anodic oxidation of BP in the presence of dA formed BP-6-N7Ade.

Electrochemical oxidation of BP in the presence of adenine (Figure 2) has led to the formation of two new depurinating adducts, BP-6-N1Ade (52%) and BP-6-N3Ade (5.6%), in addition to BP-6-N7Ade (1.7%). The NMR spectrum of BP-6-N7Ade was identical to that reported previously (12).

Elucidation of the structure of the two new depurinating adducts is based on several lines of evidence provided from their NMR spectra. In the spectra of BP-6-N3Ade (Figure 3A) and BP-6-N1Ade (Figure 3B), the upfield shift of the resonance doublets corresponding to the protons 5-H and 7-H suggests that substitution in the BP moiety occurs at C-6. The absence of the characteristic singlet signal corresponding to the proton at C-6 proves the substitution at this position. Assignments of the other aromatic protons were made by using COSY and by comparison with the NMR spectrum of the parent compound, BP. The broad singlet at 7.59 ppm (Figure 3A), which is exchangeable in D<sub>2</sub>O, corresponds to the resonance of the 6-NH<sub>2</sub> protons of the adenine moiety, indicating that substitution did not occur at the amino group. Similarly, substitution did not occur at the amino group of the proposed BP-6-N1Ade adduct structure (Figure 3B). In the latter case, the two protons are

shifted downfield and are split into two resonance signals at 8.35 and 8.45 ppm. This is due to the effect of the bulky BP moiety substituted in the ortho position, N-1, hindering the rotation of the amino group with the two protons in different magnetic environments. A similar effect has also been observed for the N1Ade adduct of DB[a,*f*]P.<sup>2</sup> Confirmation of the structures of the two isomeric adducts arises from the assignment of the 8-H and 2-H proton resonances of the adenine moiety by NOE analysis in BP-6-N3Ade. In fact, irradiation of the N<sup>6</sup>-amino group shows a selective NOE enhancement of the 2-H signal of adenine. It is known that ortho substitution of alkyl groups at N-9, as in deoxyadenosine (8.34 ppm, not shown), or at N-7, as in BP-6-N7Ade [8.68 ppm (12)], deshields the 8-H proton. The same deshielding effect is observed in the 2-H signal of adenine in both of the adducts, BP-6-N3Ade and BP-6-N1Ade (8.60 and 8.68 ppm, respectively, Figure 3), compared to 8.07 ppm for adenine itself (not shown). This suggests that substitution occurs adjacent to 2-H in the case of each adduct, and this is consistent with the structural assignments.

**Identification of DNA Adducts.** Adducts of BP formed *in vitro* were obtained by microsomal activation of BP and BP-7,8-dihydrodiol, or by direct reaction of *anti*-BPDE with DNA. In addition, BP was activated by HRP as a model for formation of adducts by one-electron oxidation. The profiles of adducts obtained *in vitro* were compared with the adducts formed when mouse skin was treated with BP, BP-7,8-dihydrodiol, or *anti*-BPDE. Identification of the depurinating adducts previously detected was achieved by coelution with authentic adducts in two solvent systems on HPLC. Newly detected adducts were preliminarily identified by coelution with standard adducts, and proof of structure was obtained by FLNS.

When BP was activated by HRP in the presence of DNA, the previously observed depurinating adducts, BP-6-C8Gua, BP-6-N7Gua, and BP-6-N7Ade (3, 5), were confirmed (Table 1). In addition, the BP-6-N3Ade adduct was identified by coelution in two HPLC solvent systems, followed by FLNS analysis. BP-6-N1Ade was not observed as expected because of the inaccessibility of the N-1 position in DNA. Identification of BP-6-N3Ade by FLN spectroscopy is illustrated in Figure 4. The top spectrum is that of the authentic standard, excited at 398.00 nm; the bottom spectrum is that of the corresponding HPLC fraction collected from the HRP-catalyzed reaction. Comparison of the vibronic frequencies and the relative intensity distribution shows that the spectra are identical. Matching spectra were also obtained at other excitation wavelengths (not shown).

In the microsomal activation of BP in the presence of DNA, the depurinating adducts previously identified, BP-6-C8Gua, BP-6-N7Gua, BP-6-N7Ade, and BPDE-10-N7Ade (4, 5), were confirmed (Table 1). BPDE-10-N7Gua was newly identified, whereas the one-electron oxidation adduct BP-6-N3Ade, obtained with HRP activation (see above), was not detected. For microsomal activation of BP-7,8-dihydrodiol and direct reaction of *anti*-BPDE with DNA, the depurinating adduct BPDE-10-N7Ade was confirmed and BPDE-10-N7Gua was detected. The major stable adduct formed from BP, BP-7,8-dihydrodiol, or *anti*-BPDE was BPDE-10-N<sup>2</sup>dG (Table 1).

In the study of mouse skin treated with BP, the presence of the previously reported depurinating adducts,

<sup>2</sup> Unpublished results, Cavalieri et al.

Table 1. Quantitation of Biologically-Formed BP-DNA Adducts<sup>a</sup>

biological system	total adducts, $\mu\text{mol/mol}$ of DNA-P	stable adducts, $\mu\text{mol/mol}$ of DNA-P		depurinating adducts, $\mu\text{mol/mol}$ of DNA-P						ratio of depurinating/stable adducts		
		BPDE-10-N <sup>7</sup> G	unidentified	total stable adducts	BP-6-N7Gua	BP-6-C8Gua	BP-6-N3Ade	BP-6-N7Ade	BPDE-10-N7Gua		BPDE-10-N7Ade	total depurinating adducts
HRP												
BP	17.8		7.1 <sup>c</sup>	7.1 (39)	0.8 (5) <sup>b</sup>	1.8 (10)	4.2 (24)	3.9 (22)		10.7 (61)	1.5	
microsomes												
BP	10.4	2.7 (26)	0.6 <sup>c</sup> (6)	3.3 (32)	1.2 (12)	1.5 (14)	<0.05	4.0 (38)	0.2 (2)	7.1 (68)	2.1	
BP 7,8-dihydrodiol	100	90 (90)	2.5 <sup>d</sup> (3)	92 (93)					1.8 (2)	7.1 (7)	0.1	
anti-BPDE	199	191 (96)	4.8 <sup>e</sup> (2)	196 (98)					1.9 (1)	3.1 (2)	0.02	
mouse skin												
BP	2.09	0.49 (23)	0.13 <sup>d</sup> (6)	0.62 (29)	0.20 (10)	0.70 (34)	<0.05	0.45 (22)	0.05 (2)	1.47 (71)	2.5	
BP 7,8-dihydrodiol	3.14	1.90 (61)	0.07 <sup>f</sup> (2)	1.97 (63)					0.37 (12)	1.17 (37)	0.6	
anti-BPDE	48	47 (98.1)	0.3 <sup>e</sup> (0.6)	47 (98.7)					0.07 (0.1)	0.62 (1.3)	0.01	

<sup>a</sup> Values are the average of determinations on two preparations. The amount of each adduct varied between 10% and 25% in the two preparations, with larger variations with the minor adducts. In vitro incubations, the concentration of BP, BP-7,8-dihydrodiol, or anti-BPDE was 80  $\mu\text{M}$ . Mouse skin was treated with 200 nmol of BP, BP-7,8-dihydrodiol, or anti-BPDE. <sup>b</sup> Number of parentheses is percentage of total adducts. <sup>c</sup> 4 adduct spots. <sup>d</sup> 1 adduct spots. <sup>e</sup> 3 adduct spots. <sup>f</sup> 2 adduct spots.

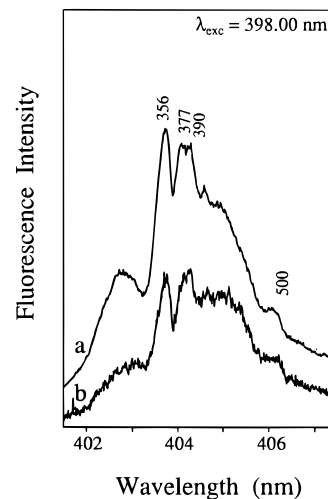


**Figure 4.** FLNS identification of BP-6-N3Ade. Curve a: spectrum of synthetic standard; curve b: spectrum of corresponding HPLC fraction, isolated from HRP-catalyzed in vitro reaction. Solvent matrix: water/glycerol/ethanol (40:40:20);  $\lambda_{\text{exc}} = 398.00 \text{ nm}$ ;  $T = 4.2 \text{ K}$ . Peaks are labeled with their excited-state vibrational frequencies.

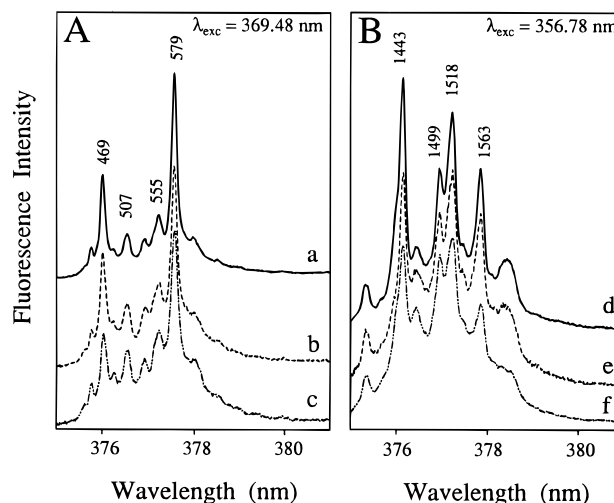


**Figure 5.** FLNS identification of BPDE-10-N7Gua, using laser excitation at 369.48 nm (frame A) or at 356.78 nm (frame B). Curves a and d: spectra of synthetic standard; curves b and e: corresponding HPLC fraction isolated from microsome-catalyzed in vitro system reacted with BP-7,8-dihydrodiol; curves c and f: corresponding HPLC fraction isolated from mouse skin reacted with BP-7,8-dihydrodiol. Solvent matrix: water/glycerol (50:50);  $T = 4.2 \text{ K}$ . Peaks are labeled with their excited-state vibrational frequencies.

BP-6-N7Gua, BP-6-C8Gua, and BP-6-N7Ade ( $\delta$ ), was confirmed, and two additional adducts, BPDE-10-N7Ade and BPDE-10-N7Gua, formed via the diol epoxide pathway, were also detected (Table 1). Only stable adducts were previously detected in mouse skin treated with BP-7,8-dihydrodiol or anti-BPDE ( $\delta$ ). In this study, both the depurinating BPDE-10-N7Ade and BPDE-10-N7Gua adducts were observed following treatment with the dihydrodiol or the diol epoxide (Table 1).

The newly detected depurinating adduct formed via the diol epoxide pathway, BPDE-10-N7Gua, was preliminarily identified by coelution with authentic standard in two different HPLC solvent systems, and its structure was definitively proven by FLN spectroscopy with excitation at various wavelengths. The results obtained at 369.48 and 356.78 nm are presented in Figure 5, panels A and B, respectively. The top spectra a and d represent the

BPDE-10-N7Gua standard, whereas the middle spectra b and e represent the adduct obtained from microsomal activation of BP-7,8-dihydrodiol, and the bottom spectra c and f were obtained for the corresponding fraction from mouse skin treated with BP-7,8-dihydrodiol. The excited-state vibrational frequencies and the relative intensities are identical in all cases, confirming the preliminary identification of this adduct based on HPLC retention times. The high resolution FLN spectra are sufficiently selective to allow for distinction between these adducts and other BPDE derivatives bound to N7Ade, N<sup>6</sup>dA, or N<sup>2</sup>dG. Comparing the FLN spectra at various excitation wavelengths with those of other BPDE adducts of known stereochemistry, the vibronic frequency pattern is similar to that of *trans-anti*-BPDE adducts (18), but very different from that of *cis-anti*-BPDE adducts (18) or adducts derived from *syn*-BPDE (19). Therefore, it is concluded that the BPDE-10-N7Gua adduct identified in this study has the *trans-anti* stereochemistry. Finally, it should be mentioned that low-temperature fluorescence spectroscopy also showed a high purity of both the BPDE-10-N7Gua and BP-6-N3Ade (see above) adduct fractions. No sign of coelution with other compounds was observed, neither under selective FLN conditions nor when more general excitation at 308 nm and low-resolution detection over a wide wavelength range and various delay times for the observation window were employed.

**Quantitation of DNA Adducts.** In the HRP experiment, the amount of BP-6-N7Ade had been previously overestimated (5, 6); however, the newly detected BP-6-N3Ade plus BP-6-N7Ade constituted approximately the same relative amount of depurinating adenine adducts (Table 1), and the ratio of depurinating adenine vs guanine adducts was 3, similar to previous experiments (5, 6). The ratio between depurinating and stable adducts was also similar to those found before (5, 6).

When BP was activated by microsomes in the presence of DNA, BP-6-N3Ade was not detected. The total amount of depurinating adducts (68%, Table 1) was less than previously found, 81% (5) and 77% (6), because the amount of BP-6-N7Ade had been overestimated. The newly detected BPDE-10-N7Gua was found in approximately the same amount as BPDE-10-N7Ade (Table 1).

For BP-7,8-dihydrodiol and *anti*-BPDE, the amount used in vitro (80  $\mu$ M) was equimolar to the amount of BP, whereas in previous experiments the two metabolites were used at 15  $\mu$ M (5, 6). This change led to much larger amounts of the stable BPDE-10-N<sup>2</sup>dG adduct (Table 1). With BP-7,8-dihydrodiol, the amounts of the depurinating adducts, BPDE-10-N7Ade and BPDE-10-N7Gua, were much larger than with BP and, in fact, equaled the total amount of depurinating adducts found with BP. Three times as much BPDE-10-N7Ade as BPDE-10-N7Gua was found. With *anti*-BPDE, the amounts of both depurinating adducts were larger compared to BP, but the increase in BPDE-10-N7Ade was not as great as with the dihydrodiol (Table 1).

In the mouse skin experiment with BP, most of the adducts were depurinated (71%), including small amounts formed from the diol epoxide (Table 1). In contrast, treatment of mouse skin with BP-7,8-dihydrodiol or *anti*-BPDE produced a majority of stable adducts, primarily BPDE-10-N<sup>2</sup>dG (61% or 98%, respectively). Treatment with BP, BP-7,8-dihydrodiol, or *anti*-BPDE yielded a total of 1.47 (100%), 1.17 (80%), or 0.62 (42%)  $\mu$ mol of depurinating adducts/mol of DNA-P, respectively. The total amount of the depurinating adducts BPDE-10-N7Gua

and BPDE-10-N7Ade was 10 times larger compared to BP for the dihydrodiol and 6 times larger for the diol epoxide. With BP, about twice as many guanine as adenine depurinating adducts was formed; BP-7,8-dihydrodiol afforded twice as many adenine as guanine depurinating adducts, and *anti*-BPDE, 8 times as many (Table 1). Overall, activation by microsomes and in mouse skin produced similar amounts of depurinating adducts for BP and BP-7,8-dihydrodiol, whereas *anti*-BPDE produced less than half as much.

**Relationship between Depurinating BP-DNA Adducts and *ras* Mutations in Mouse Skin Papillomas.** Depurinating adducts of BP and BP-7,8-dihydrodiol are formed in similar amounts (Table 1), although for BP, the depurinating adducts are predominantly formed by one-electron oxidation and only a small amount is formed by the diol epoxide pathway. *anti*-BPDE, instead, produces fewer depurinating adducts than its precursors. Stable adducts of these three compounds are mainly BPDE-10-N<sup>2</sup>dG, and the ratio of the amount of stable adducts formed by BP, BP-7,8-dihydrodiol, and *anti*-BPDE is 1 to 3 to 80, respectively.

The tumorigenicity of BP and BP-7,8-dihydrodiol in mouse skin by initiation-promotion and repeated application shows that these two compounds have similar activity (20-25). The (-)-BP-7,8-dihydrodiol enantiomer, the proximate metabolite leading to the most active (+)-*anti*-BPDE, has potency similar to BP in mouse skin (26, 27). The carcinogenic activity of the (+)-*anti*-BPDE by repeated application (24) and initiation-promotion (27) in mouse skin revealed that this compound is considerably weaker as a carcinogen than BP. Thus, it is evident that carcinogenicity correlates with the level of depurinating adducts, but not with stable adducts.

The level of depurinating adducts of BP also correlates with mutations found in the Harvey-*ras* oncogene in mouse skin papillomas initiated with this compound (10). Depurinating guanine and adenine adducts comprise 46% and 25%, respectively, of the total BP-DNA adducts formed in mouse skin. *Ras* mutations found in DNA from 54% of the papillomas exhibit G  $\rightarrow$  T transversions in codon 13, and 15% exhibit A  $\rightarrow$  T transversions in codon 61 (10). Similar results were previously obtained by Colapietro *et al.* (28). Furthermore, six stereoisomers of the stable BPDE-N<sup>6</sup>dA adduct were linked at position 2 of human N-*ras* codon 61 (CAA) in an 11-base oligonucleotide. However, in *Escherichia coli* this adduct did not induce the expected A  $\rightarrow$  T transversions found in codon 61 of mouse skin tumors initiated by BP, but only A  $\rightarrow$  G transitions (29). This result is consistent with the view that the mutations found in the *ras* oncogene in mouse skin papillomas derive from depurinating adducts, rather than stable adducts. Thus, the depurinating adducts formed by BP appear to be the key adducts leading to tumor initiation. A relationship between depurinating adducts and *ras* mutations has also been observed for 7,12-dimethylbenz[*a*]anthracene, DB[*a*],JP, and some of its oxygenated metabolites (10). By using the profiles of the depurinating adducts formed in mouse skin after treatment with BP-7,8-dihydrodiol or *anti*-BPDE, namely, BPDE-10-N7Ade and BPDE-10-N7Gua, it will be possible to seek correlation with H-*ras* mutations in mouse skin papillomas induced by these two metabolites.

**Acknowledgment.** We thank Dr. G. P. Casale for valuable discussion of this research. We gratefully acknowledge support from USPHS, Grant P01 CA49210.

Core support to the Eppley Institute was provided by Grant CA36727 from the National Cancer Institute.

## References

- Cavalieri, E. L., and Rogan, E. G. (1992) The approach to understanding aromatic hydrocarbon carcinogenesis. The central role of radical cations in metabolic activation. *Pharmacol. Ther.* **55**, 183–199.
- Cavalieri, E. L., and Rogan, E. G. (1995) Central role of radical cations in metabolic activation of polycyclic aromatic hydrocarbons. *Xenobiotica* **25**, 677–688.
- Rogan, E., Cavalieri, E., Tibbels, S., Cremonesi, P., Warner, C., Nagel, D., Tomer, K., Cerny, R., and Gross, M. (1988) Synthesis and identification of benzo[a]pyrene-guanine nucleoside adducts formed by electrochemical oxidation and horseradish peroxidase-catalyzed reaction of benzo[a]pyrene with DNA. *J. Am. Chem. Soc.* **110**, 4023–4029.
- Cavalieri, E. L., Rogan, E. G., Devanesan, P. D., Cremonesi, P., Cerny, R. L., Gross, M. L., and Bodell, W. J. (1990) Binding of benzo[a]pyrene to DNA by cytochrome P-450-catalyzed one-electron oxidation in rat liver microsomes and nuclei. *Biochemistry* **29**, 4820–4827.
- Devanesan, P. D., RamaKrishna, N. V. S., Todorovic, R., Rogan, E. G., Cavalieri, E. L., Jeong, H., Jankowiak, R., and Small, G. J. (1992) Identification and quantitation of benzo[a]pyrene-DNA adducts formed by rat liver microsomes *in vitro*. *Chem. Res. Toxicol.* **5**, 302–309.
- Rogan, E. G., Devanesan, P. D., RamaKrishna, N. V. S., Higginbotham, S., Padmavathi, N. S., Chapman, K., Cavalieri, E. L., Jeong, H., Jankowiak, R., and Small, G. J. (1993) Identification and quantitation of benzo[a]pyrene-DNA adducts formed in mouse skin. *Chem. Res. Toxicol.* **6**, 356–363.
- RamaKrishna, N. V. S., Devanesan, P. D., Rogan, E. G., Cavalieri, E. L., Jeong, H., Jankowiak, R., and Small, G. J. (1992) Mechanism of metabolic activation of the potent carcinogen 7,12-dimethylbenz[a]anthracene. *Chem. Res. Toxicol.* **5**, 220–226.
- Devanesan, P. D., RamaKrishna, N. V. S., Padmavathi, N. S., Higginbotham, S., Rogan, E. G., Cavalieri, E. L., Marsch, G. A., Jankowiak, R., and Small, G. J. (1993) Identification and quantitation of 7,12-dimethylbenz[a]anthracene-DNA adducts formed in mouse skin. *Chem. Res. Toxicol.* **6**, 364–371.
- Li, K.-M., Todorovic, R., Rogan, E. G., Cavalieri, E. L., Ariese, F., Suh, M., Jankowiak, R., and Small, G. J. (1995) Identification and quantitation of dibenzo[a,h]pyrene-DNA adducts formed by rat liver microsomes *in vitro*: Preponderance of depurinating adducts. *Biochemistry* **34**, 8043–8049.
- Chakravarti, D., Pelling, J. C., Cavalieri, E. L., and Rogan, E. G. (1995) Relating aromatic hydrocarbon-induced DNA adducts and c-Harvey-ras mutations in mouse skin papillomas: The role of apurinic sites. *Proc. Natl. Acad. Sci. U.S.A.* **92**, 10422–10426.
- NIH Guidelines for the Laboratory Use of Chemical Carcinogens (1981) NIH Publication No. 81-2385, U.S. Government Printing Office, Washington, DC.
- RamaKrishna, N. V. S., Gao, F., Padmavathi, N. S., Cavalieri, E. L., Rogan, E. G., Cerny, R. L., and Gross, M. L. (1992) Model adducts of benzo[a]pyrene and nucleosides formed from its radical cation and diol epoxide. *Chem. Res. Toxicol.* **5**, 293–302.
- Cremonesi, P., Rogan, E., and Cavalieri, E. (1992) Correlation studies of anodic peak potentials and ionization potentials for polycyclic aromatic hydrocarbons. *Chem. Res. Toxicol.* **5**, 346–355.
- Bodell, W. J., Devanesan, P. D., Rogan, E. G., and Cavalieri, E. L. (1989) <sup>32</sup>P-Postlabeling analysis of benzo[a]pyrene-DNA adducts formed *in vitro* and *in vivo*. *Chem. Res. Toxicol.* **2**, 312–315.
- Burton, K. (1956) A study of the conditions and mechanism of the diphenylamine reaction for the colorimetric estimation of deoxyribonucleic acid. *Biochem. J.* **62**, 315–323.
- Jankowiak, R., and Small, G. J. (1989) Fluorescence line-narrowing spectroscopy in the study of chemical carcinogenesis. *Anal. Chem.* **61**, 1023A–1032A.
- Jankowiak, R., and Small, G. J. (1991) Fluorescence line-narrowing: a high-resolution window on DNA and protein damage from chemical carcinogens. *Chem. Res. Toxicol.* **4**, 256–269.
- Suh, M., Ariese, F., Small, G. J., Jankowiak, R., Liu, T.-M., and Geacintov, N. E. (1995) Conformational studies of the (+)-*trans*, (-)-*trans*, (+)-*cis*, and (-)-*cis* adducts of *anti*-benzo[a]pyrene diol epoxide to N<sup>2</sup>-dG in duplex oligonucleotides using polyacrylamide electrophoresis and low-temperature fluorescence spectroscopy. *Biophys. Chem.* **56**, 281–296.
- Jankowiak, R., Lu, P., Small, G. J., Nishimoto, M., Varanasi, U., Kim, S. K., and Geacintov, N. E. (1990) Fluorescence line-narrowing spectrometry: a versatile tool for the study of chemically initiated carcinogenesis. *J. Pharm. Biomed. Anal.* **8**, 113–121.
- Chouroulinkov, I., Gentil, A., Grover, P. L., and Sims, P. (1976) Tumor-initiating activities on mouse skin of dihydrodiols derived from benzo[a]pyrene. *Br. J. Cancer* **34**, 523–532.
- Slaga, T. J., Viaje, A., Berry, D. L., and Bracken, W. (1976) Skin tumor initiating ability of benzo[a]pyrene 4,5-, 7,8-, and 7,8-diol-9,10-epoxides and 7,8-diol. *Cancer Lett.* **2**, 115–122.
- Levin, W., Wood, A. W., Yagi, H., Dansette, P. M., Jerina, D. M., and Conney, A. H. (1976) Carcinogenicity of benzo[a]pyrene 4,5-, 7,8- and 9,10-oxides on mouse skin. *Proc. Natl. Acad. Sci. U.S.A.* **73**, 243–247.
- Levin, W., Wood, A. W., Yagi, H., Jerina, D. M., and Conney, A. H. (1976) ( $\pm$ )-*trans*-7,8-Dihydroxy-7,8-dihydrobenzo[a]pyrene: A potent skin carcinogen when applied topically to mice. *Proc. Natl. Acad. Sci. U.S.A.* **73**, 3867–3871.
- Levin, W., Wood, A. W., Wislocki, P. G., Kapitulnik, J., Yagi, H., Jerina, D. M., and Conney, A. H. (1977) Carcinogenicity of benzo[a]pyrene derivatives of benzo[a]pyrene on mouse skin. *Cancer Res.* **37**, 3356–3361.
- Cavalieri, E., Sinha, D., and Rogan, E. (1980) Rat mammary gland versus mouse skin: Different mechanisms of activation of aromatic hydrocarbons. In *Polynuclear Aromatic Hydrocarbons: Chemistry and Biological Effects* (Bjorseth, A., and Dennis, A. J., Eds.) pp 215–231, Battelle Press, Columbus, OH.
- Levin, W., Wood, A. W., Chang, R. L., Slaga, T. J., Yagi, H., Jerina, D. M., and Conney, A. H. (1977) Marked differences in the tumor-initiating activity of optically pure (+) and (-)-*trans*-7,8-dihydroxy-7,8-dihydrobenzo[a]pyrene on mouse skin. *Cancer Res.* **37**, 2721–2725.
- Slaga, T. J., Bracken, W. M., Viaje, A., Levin, W., Yagi, H., Jerina, D. M., and Conney, A. H. (1977) Comparison of the tumor-initiating activities of benzo[a]pyrene arene oxides and diol-epoxides. *Cancer Res.* **37**, 4130–4133.
- Colapietro, A.-M., Goodell, A. L., and Smart, R. C. (1993) Characterization of benzo[a]pyrene-initiated mouse skin papillomas for Ha-ras mutations and protein kinase C levels. *Carcinogenesis* **14**, 2289–2295.
- Chary, P., Latham, G. J., Robberson, D. L., Kim, S. J., Han, S., Harris, C. M., Harris, T. M., and Lloyd, R. S. (1995) *In vivo* and *in vitro* replication consequences of stereoisomeric benzo[a]pyrene-7,8-dihydrodiol 9,10-epoxide adducts on adenine N<sup>6</sup> at the second position of N-ras codon 61. *J. Biol. Chem.* **270**, 4990–5000.

TX960004A